Living Cells as Test Tubes

X. Sunney Xie *et al.*

Science **312**, 228 (2006);
DOI: 10.1126/science.1127566

Science (print ISSN 0036-8075; online ISSN 1095-9203) is published weekly, except the last week in December, by the American Association for the Advancement of Science, 1200 New York Avenue NW, Washington, DC 20005.

10. R. Ishima, J. M. Louis, D. A. Torchia, *J. Mol. Biol.* **305**, 515 (2001).
11. M. J. Grey, C. Y. Wang, A. G. Palmer, *J. Am. Chem. Soc.* **125**, 14324 (2003).
12. F. A. A. Mulder, A. Mittermaier, B. Hon, F. W. Dahlquist, L. E. Kay, *Nat. Struct. Biol.* **8**, 932 (2001).
13. M. Wolf-Watz *et al.*, *Nat. Struct. Mol. Biol.* **11**, 945 (2004).
14. E. Z. Eisenmesser *et al.*, *Nature* **438**, 117 (2005).
15. G. Lipari, A. Szabo, *J. Am. Chem. Soc.* **104**, 4546 (1982).
16. T. Bremi, R. Brüschweiler, *J. Am. Chem. Soc.* **119**, 6672 (1997).
17. P. Pelupessy, S. Ravindranathan, G. Bodenhausen, *J. Biomol. NMR* **25**, 265 (2003).
18. P. Lundstrom, F. A. Mulder, M. Akke, *Proc. Natl. Acad. Sci. U.S.A.* **102**, 16984 (2005).
19. T. Wang, K. K. Frederick, T. I. Igumenova, A. J. Wand, E. R. Zuiderweg, *J. Am. Chem. Soc.* **127**, 828 (2005).
20. D. M. LeMaster, D. M. Kushlan, *J. Am. Chem. Soc.* **118**, 9255 (1996).
21. D. R. Muhandiram, T. Yamazaki, B. D. Sykes, L. E. Kay, *J. Am. Chem. Soc.* **117**, 11536 (1995).
22. K. Lindorff-Larsen, R. B. Best, M. A. Depristo, C. M. Dobson, M. Vendruscolo, *Nature* **433**, 128 (2005).
23. N. Tjandra, A. Bax, *Science* **278**, 1111 (1997).
24. J. R. Tolman, J. M. Flanagan, M. A. Kennedy, J. H. Prestegard, *Nat. Struct. Biol.* **4**, 292 (1997).
25. G. M. Clore, C. D. Schwieters, *Biochemistry* **43**, 10678 (2004).
26. J. Meiler, J. J. Prompers, W. Peti, C. Griesinger, R. Bruschweiler, *J. Am. Chem. Soc.* **123**, 6098 (2001).
27. J. J. Chou, D. A. Case, A. Bax, *J. Am. Chem. Soc.* **125**, 8959 (2003).
28. G. Bouvignies *et al.*, *Proc. Natl. Acad. Sci. U.S.A.* **102**, 13885 (2005).
29. K. Pervushin, R. Riek, G. Wider, K. Wüthrich, *Proc. Natl. Acad. Sci. U.S.A.* **94**, 12366 (1997).
30. R. Horst *et al.*, *Proc. Natl. Acad. Sci. U.S.A.* **102**, 12748 (2005).
31. R. Sprangers, A. Gribun, P. M. Hwang, W. A. Houry, L. E. Kay, *Proc. Natl. Acad. Sci. U.S.A.* **102**, 16678 (2005).

10.1126/science.1124964

PERSPECTIVE

Living Cells as Test Tubes

X. Sunney Xie,* Ji Yu, Wei Yuan Yang

The combination of specific probes and advanced optical microscopy now allows quantitative probing of biochemical reactions in living cells. On selected systems, one can detect and track a particular protein with single-molecule sensitivity, nanometer spatial precision, and millisecond time resolution. Metabolites, usually difficult to detect, can be imaged and monitored in living cells with coherent anti-Stokes Raman scattering microscopy. Here, we describe the application of these techniques in studying gene expression, active transport, and lipid metabolism.

Much of our quantitative understanding of molecular reactions in cells has come from traditional biochemistry—experiments done in test tubes with purified biomolecules. Although this approach is extremely productive, we understand that the milieu of the cell is fundamentally different from an in vitro solution in several ways: (i) DNA, many mRNA molecules, and some enzymes exist in low copy numbers and participate in stochastic reaction events in the cell that are hidden in test tubes with large numbers of molecules. (ii) Reactions are often at nonequilibrium steady state in the cell, with a constant supply of free energy and reactants. (iii) Many reactions are coupled in the cell, resulting in networks of complex interactions. Consequently, a biochemical reaction in a single cell could have different thermodynamic and kinetic properties from the same biochemical reaction in a test tube. The challenge now is to observe the biochemical reactions in living cells, and techniques are in place to do this in selected systems. Central to these techniques is optical imaging, which offers millisecond time resolution and nanometer spatial precision, single-molecule sensitivity, and most importantly, biochemical specificity. Here, we highlight advances that allow investigation of gene expression, active transport, and metabolism in living cells.

Department of Chemistry and Chemical Biology, Harvard University, Cambridge, MA 02138, USA.

*To whom correspondence should be addressed. E-mail: xie@chemistry.harvard.edu

In an individual cell, gene expression is a single-molecule problem. On genomic DNA, a particular gene only exists in one (or a few) copy, switching on and off stochastically to regulate biological functions [for a review, see (*1*)]. Gene expression has been studied by biochemical assays, such as Northern and Western blotting, polymerase chain reaction, and more recently, DNA arrays and mass spectrometry. However, these techniques are not sensitive enough to allow single-cell analysis of genes that are expressed at low levels. Furthermore, these ensemble-averaged methods often mask stochastic gene expression events. Single-molecule experiments in vitro have provided valuable insight into the mechanisms of gene expression machines (*2*–*4*). The next frontier will carry out single-molecule studies in individual living cells.

Imaging of gene expression at a single-molecule level in living cells has been made possible by two developments. At the transcriptional level, single mRNA molecules were detected and tracked in a living cell using multiple copies of a fluorescent mRNA binding protein (*5*, *6*). At the translational level, we have tracked expression of single-protein molecules using a fast-maturing and membrane-targeting yellow fluorescent protein (YFP) (Venus) as a reporter (*7*).

Immobilizing the fluorescent protein reporter on the cell membrane (*7*, *8*) overcame the difficulty in detecting single-protein molecules inside the cytoplasm; the fluorescence distributes throughout the cell because of fast protein diffusion during the image acquisition time and drops below the strong cellular autofluorescence. We monitored repressed expression from the *lac* promoter in *Escherichia coli* (Fig. 1A) and showed that protein expression occurs in small bursts (Fig. 1B), each originating from multiple ribosomes on an mRNA molecule. The protein copy numbers within a burst adhered to a geometric distribution (*7*), which was verified with the use of a different reporter (*9*). These assays provided quantitative details about the stochastic fluctuations in gene expression.

Is there a way to detect a single cytoplasmic protein molecule? The answer is yes, by extending the idea of detection by immobilization. We borrowed a method from strobe photography, which makes it possible to take a sharp picture of a bullet going through an apple (Fig. 1C). The sharpness is achieved because the light flash is so short that the bullet does not move far during the flash. Likewise, we applied an intense laser exposure for a very short duration (~300 μs), during which a protein reporter does not diffuse beyond the diffraction-limited spot. Figure 1D shows detection of single red fluorescent proteins [tdTomato (*10*)] in *E. coli* cytoplasm with a high signal-to-background ratio. The method could be used, for example, to determine the cellular concentration of a weakly expressed protein without calibration. To further develop this method, we need reporters with high photostability and better-controlled photochemistry.

The next step is to probe the expression of multiple genes simultaneously with the use of different colors of reporters (*10*) in order to study their interactions. In addition to transcription and translation, similar live-cell single-molecule assays offer the prospect of studying cellular processes, such as cell signaling (*11*), protein folding, DNA replication, and RNA trafficking (*5*, *12*).

No less important than gene expression is energy transduction in living cells. Motor proteins convert chemical energy in the form of adenosine 5′-triphosphate (ATP) into mechanical work. Kinesin and dynein motors transport organelles along microtubules in opposite directions. Much has been learned about these motors at the single-

molecule level through in vitro experiments with mechanical manipulation and optical detection (*13*, *14*). However, little is known about the workings of motors at the single-molecule level in vivo.

Last year, two groups reported the observation of individual steps of molecular motors in living cells with nanometer spatial precision and millisecond time resolution with the use of sensitive high-speed cameras (*15*, *16*). A key technical concept is that even though diffraction results in a fluorescent spot size of ~270 nm, one can determine the centroid position of an isolated fluorophore with nanometer spatial resolution (*17*–*19*), provided that the optical signal is sufficiently bright. This idea was first applied in vitro to resolve the individual steps of molecular motors (*20*). Presenting an additional challenge, in vivo motor speeds are faster because the cell's ATP concentrations are higher than those used for in vitro measurements. Thus, higher time resolution is required to resolve individual steps.

In the example from our laboratory, Nan *et al.* achieved submillisecond time resolution in resolving the discrete nanometer steps of molecular motors by tracking the motion of endocytic vesicles (*16*) containing quantum dots (QDs). QDs are extremely bright (*21*, *22*), and after introduction into mouse fibroblast cells by endocytosis, the QD-containing vesicle moves on microtubules (Fig. 2A). Steps of 8 nm, each corresponding to a stochastic ATP hydrolysis event, are resolved (Fig. 2B), as evidenced by the 8-nm spacings in the pairwise correlation function (Fig. 2C). Stepwise movements of the QD-containing vesicle are seen in both directions along the microtubule, with some showing steps larger than 8 nm and others exhibiting reversible steps. These observations raise interesting questions regarding how multiple copies and types of motors work collectively in a living cell. These live-cell motility assays are yielding new dynamic information and will be even more productive if force sensing (*23*, *24*) and mechanical manipulation of motors, similar to those implemented in vitro, can be realized in living cells.

Unlike proteins that can often be labeled without altering function, the majority of metabolites are small organic molecules that are difficult to label for imaging without altering their cellular behavior. Raman scattering offers a way to image metabolites without the need for exogenous labels, as it probes intrinsic molecular vibrational frequencies. For example, the Raman spectra of two fatty acid species, eicosapentaenoic acid (EPA) and fully deuterated oleic acid (OA), have two distinct peaks arising from strong $–CH_2$ and $–CD_2$ stretching vibrations contained within the respective acyl-chains of the two fatty acid molecules (Fig. 3A).

For living cells, however, Raman signals are so weak that high excitation powers and long acquisition times (hours) are required to obtain useful images. A noninvasive method in live-cell and animal imaging, coherent anti-Stokes Raman

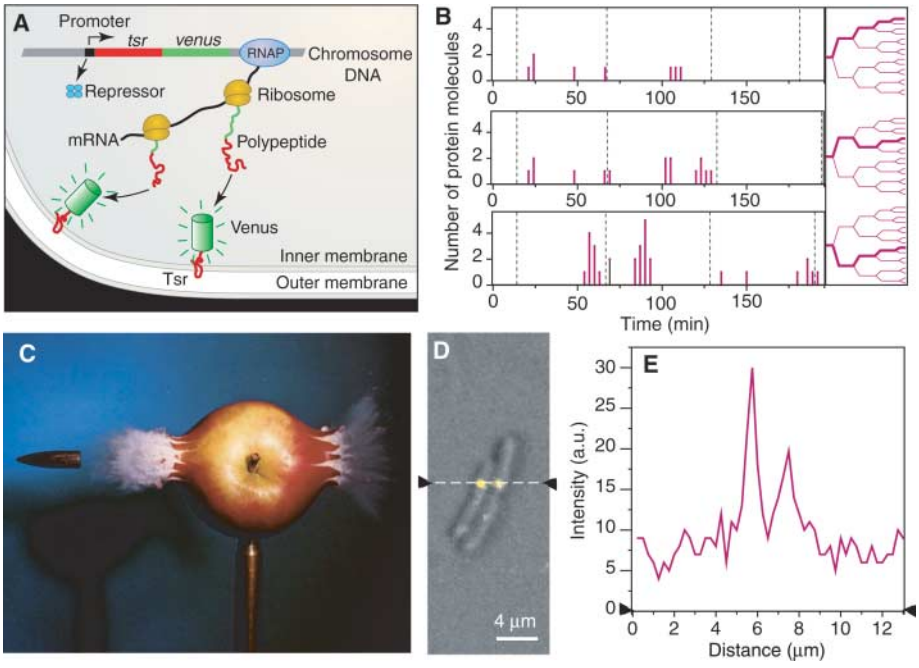

Fig. 1. Imaging protein expression in live *E. coli* cells. (**A**) When a repressor dissociates from the *lac* promoter, RNA polymerase transcribes the gene of a fusion protein Tsr-Venus into an mRNA, on which a few ribosomes bind, each making a fusion protein molecule. Tsr targets Venus, a fast-maturing YFP, to the membrane, allowing detection of Venus one molecule at a time. (**B**) Time traces of the burst production of Tsr-Venus (left) in three cell lineages (right) extracted from the time-lapse recording of protein production. Images with 100-ms exposure, followed by 1000-ms photobleaching, were taken every 3 min and the number of protein molecules synthesized since the last image was counted. The dotted lines mark the cell division times. (**C**) Image of a bullet passing through an apple (*32*), obtained using strobe photography. (**D**) Fluorescence/DIC overlay image of three *E. coli* cells, with two containing single cytoplasmic tdTomato molecules. The fluorescence image was taken with a short (300-μs) and intense (50-kW/cm^2) laser excitation. (**E**) Fluorescence signal with two distinct peaks along the line in (D) due to two single cytoplasmic tdTomato molecules. a.u., arbitrary units.

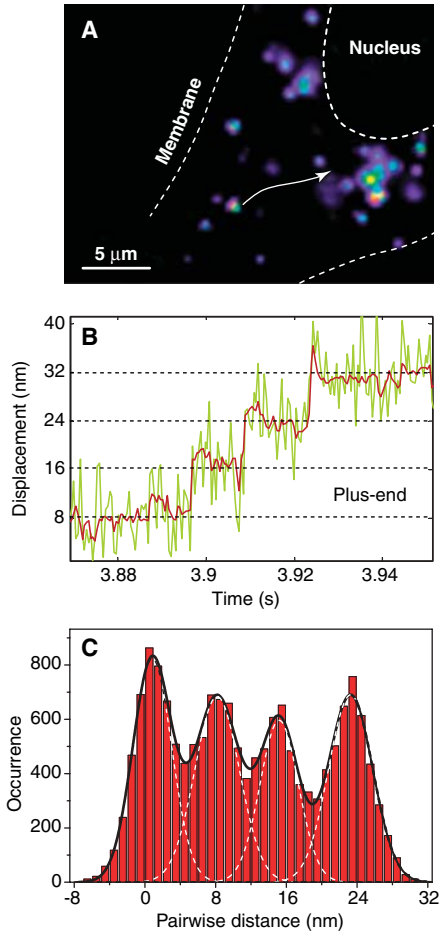

Fig. 2. Observation of individual microtubule motor steps in a live cell with endocytosed quantum dots. (**A**) Live A549 cell with QD-containing endosomes (bright dots), many of which undergo active transport by kinesin (outward movements) or dynein (inward movements, white arrow). (**B**) Displacement trajectory of a outward-going (microtubule plus-end) endosome, exhibiting stepwise movements of the underlying motor (likely kinesin). Green, raw data; red, filtered data. (**C**) Pairwise distance histogram of the filtered displacement trace in (B), with an 8-nm spacing between adjacent peaks.

scattering (CARS) microscopy provides vibrational contrast with a sensitivity that is orders of magnitude higher than conventional Raman microscopy (*25*–*27*). The technique uses two temporally and collinearly overlapped picosecond laser beams at different frequencies, ω_p and ω_s, which are tightly focused onto the sample. When $\omega_p - \omega_s$ matches the vibrational frequency of the molecular species of interest, molecular oscillators are driven coherently, resulting in a resonance-enhanced CARS signal at the anti-Stokes frequency $2\omega_p - \omega_s$. CARS is only generated at the laser focus, allowing three-dimensional sectioning, similar to two-photon fluorescence microscopy (*28*). Although CARS microscopy does not offer the penetration depth of magnetic resonance imaging (MRI), it does offer better time and spatial resolution than MRI, which is key for monitoring living cells. CARS microscopy is particularly powerful in tracking lipid metabolism, due to the large number of CH bonds in lipids.

As an example of an application of CARS microscopy, we monitored how fish oil affects the cellular biochemistry of fat molecules (*29*). It has long been realized that polyunsaturated fatty acids, such as EPA, in fish oil provide health benefits by lowering triglyceride levels. This effect prompted the Food and Drug Administration to issue a qualified health claim in 2004 for fish oil on avoiding heart disorders, diseases often associated with high lipid levels in the blood.

To distinguish the normal fatty acids (i.e., OA) from EPA, we used deuterated OA. This approach is similar to isotope tracking, historically used to identify metabolic pathways (*30*). The deuteration results in a vibrational frequency shift, from 2850 cm^{-1} for $-CH_2$ to 2105 cm^{-1} for $-CD_2$ (Fig. 3A). In cells grown with non-deuterated EPA and deuterated OA in the culturing media, we found that the two fatty acids colocalized in the lysosomes, the digestive organelles of the cell, in the form of triglycerides (Fig. 3, B to F). In contrast, OA is not incorporated into the lysosomes when EPA is absent. This provides an important assay toward the understanding of fish oil's health benefits. Future integration of fluorescence imaging of reporter proteins with CARS microscopy will lead to new understanding of metabolism at the systems level.

Currently, the sensitivity of CARS microscopy is 10^5 vibrational oscillators at the laser focus (*31*). We are working to improve the sensitivity for imaging other small molecules of low concentrations, such as drugs.

New single-molecule and metabolic imaging techniques, when combined with novel reporters and integrated into cellular assays, offer exciting possibilities for unraveling biochemistry in vivo. The application and continuous evolution of these fronts will lead to a quantitative understanding of fundamental biochemical processes in living cells.

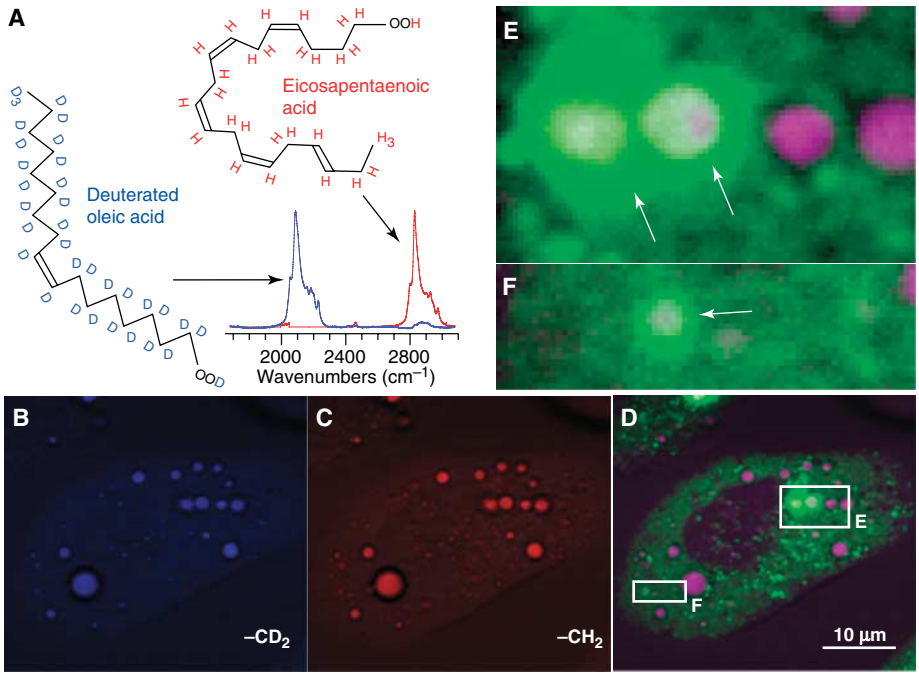

Fig. 3. Effect of fish oil on lipid metabolism studied by metabolic imaging with CARS microscopy. (**A**) Raman spectra of EPA and deuterated OA. (**B** to **F**) Live liver cells were treated with 0.4 mM EPA and 0.2 mM deuterated OA for 7.5 hours and labeled with monodansylcadaverine, a dye for staining degradative organelles. (B) CARS image tuned to $-CD_2$ (blue, deuterated OA). (C) CARS image tuned to $-CH_2$ (red, EPA). (D) Composite image of well-mixed $-CO_2$ and $-CH_2$ (purple) and two-photon fluorescence from monodansylcadaverine (green). [(E) and (F)] Zoomed-in regions in the cell where triglycerides rich in $-CH_2$ and $-CD_2$ are colocalized within degradative compartments (stained by monodansylcadaverine and indicated by arrows).

References and Notes

1. J. M. Raser, E. K. O'Shea, *Science* **309**, 2010 (2005).
2. M. D. Wang *et al.*, *Science* **282**, 902 (1998).
3. R. J. Davenport, G. J. Wuite, R. Landick, C. Bustamante, *Science* **287**, 2497 (2000).
4. S. C. Blanchard, H. D. Kim, R. L. J. Gonzalez, J. D. Puglisi, S. Chu, *Proc. Natl. Acad. Sci. U.S.A.* **101**, 12893 (2004).
5. Y. Shav-Tal *et al.*, *Science* **304**, 1797 (2004).
6. I. Golding, J. Paulsson, S. M. Zawilski, E. C. Cox, *Cell* **123**, 1025 (2005).
7. J. Yu, J. Xiao, X. Ren, K. Lao, X. S. Xie, *Science* **311**, 1600 (2006).
8. J. Deich, E. M. Judd, H. H. McAdams, W. E. Moerner, *Proc. Natl. Acad. Sci. U.S.A.* **101**, 15921 (2004).
9. L. Cai, N. Friedman, X. S. Xie, *Nature* **440**, 358 (2006).
10. N. C. Shaner, P. A. Steinbach, R. Y. Tsien, *Nature Methods* **2**, 905 (2005).
11. M. Ueda, Y. Sako, T. Tanaka, P. Devreotes, T. Yanagida, *Science* **294**, 864 (2001).
12. H. P. Babcock, C. Chen, X. Zhuang, *Biophys. J.* **87**, 2749 (2004).
13. K. Svoboda, C. F. Schmidt, B. J. Schnapp, S. M. Block, *Nature* **365**, 721 (1993).
14. R. D. Vale *et al.*, *Nature* **380**, 451 (1996).
15. C. Kural *et al.*, *Science* **308**, 1469 (2005).
16. X. Nan, P. A. Sims, P. Chen, X. S. Xie, *J. Phys. Chem. B* **109**, 24220 (2005).
17. J. Gelles, B. J. Schnapp, M. P. Sheetz, *Nature* **331**, 450 (1988).
18. E. Betzig, *Opt. Lett.* **20**, 237 (1995).
19. R. E. Thompson, D. R. Larson, W. W. Webb, *Biophys. J.* **82**, 2775 (2002).
20. A. Yildiz *et al.*, *Science* **300**, 2061 (2003).
21. M. Bruchez Jr., M. Moronne, P. Gin, S. Weiss, A. P. Alivisatos, *Science* **281**, 2013 (1998).
22. W. C. Chan, S. Nie, *Science* **281**, 2016 (1998).
23. M. A. Welte, S. P. Gross, M. Postner, S. M. Block, E. F. Wieschaus, *Cell* **92**, 547 (1998).
24. A. Ashkin, K. Schutze, J. M. Dziedzic, U. Euteneuer, M. Schliwa, *Nature* **348**, 346 (1990).
25. A. Zumbusch, G. R. Holtom, X. S. Xie, *Phys. Rev. Lett.* **82**, 4142 (1999).
26. J. X. Cheng, X. S. Xie, *J. Phys. Chem. B* **108**, 827 (2004).
27. C. L. Evans *et al.*, *Proc. Natl. Acad. Sci. U.S.A.* **102**, 16807 (2005).
28. W. Denk, J. H. Strickler, W. W. Webb, *Science* **248**, 73 (1990).
29. G. Thorne-Tjomsland *et al.*, *Mol. Biol. Cell* **14**, 104a (2003).
30. R. Schoenheimer, D. Rittenberg, *Science* **87**, 221 (1938).
31. G. Ganikhanov *et al.*, *Opt. Lett.*, in press.

32. Harold and Esther Edgerton Foundation, 2006, courtesy of Palm Press, Inc.
33. We thank current and former group members, especially X. Nan, J. Xiao, P. Chen, and P. Sims for contributing to the work summarized herein and X. Nan for providing Fig. 2. We acknowledge the fruitful collaboration on lipid metabolism with Z. Yao at the University of Ottawa, G. Thorne-Tjomsland at the University of Manitoba, and their colleagues. This work is supported by a NIH Director's Pioneer Award. The title was inspired by J. Widom's remark: "Living cells are the test tubes of the 21st century."

10.1126/science.1127566